Computational design of tissue engineering scaffolds

4

Esther Reina-Romo[1,a], *Ioannis Papantoniou*[2,3,a], *Veerle Bloemen*[2,4], *Liesbet Geris*[2,5,6]

[1]University of Seville, Department of Mechanical Engineering and Manufacturing, Seville, Spain; [2]Prometheus, LRD Division of Skeletal Tissue Engineering, KU Leuven, Leuven, Belgium; [3]Skeletal Biology & Engineering Research Center, KU Leuven, Leuven, Belgium; [4]Materials Technology TC, Campus Group T, KU Leuven, Leuven, Belgium; [5]Biomechanics Research Unit, GIGA - In silico Medicine, Université de Liège, Liège, Belgium; [6]Biomechanics Section, KU Leuven, Leuven, Belgium

4.1 Introduction

Next to in vitro and in vivo models, a third model system is increasingly used in biomedical sciences, namely in silico models. In silico refers to silicium, the basic component of computer chips, and means the use of computer modeling and simulation in the broadest sense of the word. These models can be purely data driven (empirical, black box) or they can be based on already identified mechanisms (hypothesis driven, white box).

The use of computational tools presents multiple advantages for aiding scaffold design by identifying suitable design options before laborious and costly experimental effort. Given recent advances in bioprinting and biomanufacturing technologies, which possess the required accuracy for producing scaffolds with the necessary morphometric properties, the use of in silico models becomes indispensable as a compass for rational production of tissue-engineered implants. In this chapter, we will present examples where computational models have successfully supported the design and production of scaffolds and fabrication technologies.

In this chapter, we will follow the typical technological phases of the scaffold fabrication process [1–3].

- Step 1—preprocessing: design of the scaffold. This design will take into account structural, mechanical, degradation, and mass transport properties.
- Step 2—the fabrication process.
- Step 3—postprocessing: bioreactor culture.

We will limit our discussion in all steps to the questions for which in silico models have been or are being developed. We continue the chapter with a discussion on (multiobjective) optimization strategies as the need for these approaches becomes imperative because there is a dramatic increase in both computational and experimental

[a]These authors contributed equally.

Handbook of Tissue Engineering Scaffolds: Volume One. https://doi.org/10.1016/B978-0-08-102563-5.00004-6

capacity and throughput. Finally, we end with a glance toward the regulatory aspects related to the inclusion of in silico generated evidence in dossiers submitted to the regulatory agencies. Fig. 4.1 gives a schematic summary of this outline.

4.2 Preprocessing: design of the scaffold

In this section, we present an overview of how in silico models have allowed the design and optimization of key scaffold design properties such as topology, mechanical properties, degradation, and mass transport (cf. Chapter 1 in this volume [112]). Topology, including pore shape, is a factor affecting tissue growth volume and nutrient transport. Mechanical properties affect scaffold deformation under load and, therefore, tissue stimulation and integration upon implantation. The degradability influences the release of bioactive constituents affecting the biologic state of cells surrounding scaffold struts. Finally, mass transport considerations (within scaffold struts and/or pores) are crucial for cell survival and efficient differentiation. Many of the aforementioned scaffold properties might have synergistic and/or antagonistic effects on cell function. Computational tools allow to decouple these effects and to contribute in improved understanding and hence rational use in scaffold design. Optimal combinations of the aforementioned might depend on tissue type and target organ.

4.2.1 Scaffold structural properties

In silico models can help link observed tissue-scale dynamics with unknown cellular activity [6]. Initial work by Hollister et al. [7–11] focused on the design of bone scaffolds as an optimization problem to obtain a microstructure as similar as possible (in terms of mechanical properties, porosity, pore size, etc.) to that of the implanted region. For this purpose, homogenization theory was extensively applied in their studies. In other work, mechanical properties and permeability were homogenized over a representative element of a bioceramic scaffold microstructure [12]. The obtained results were corroborated by an experimental setup showing the potential of numerical tools for the characterization of scaffold properties. A series of experimental studies in fact showed that pore geometry influences stem cell behavior [13] through various mechanisms [14]. However, the underlying mechanism regarding geometric regulation of collective cell crowding and neotissue formation was the impact of curvature [15] and specifically of its interplay with linear tension [16]. In addition, the cellular stress dictated by the scaffold geometry through local curvature translates in the secretion of prestressed extracellular matrix architectures following stress patterns [17]. Hence, instead of a random trial and error approach, various studies focused on a design approach for scaffold bioprinting whereby fundamental properties were investigated rather than trivial shapes and sizes. First single pore shapes models were used to probe the rate of infilling by cells in convex and concave surfaces [6] for simple geometries, while later on Guyot et al. [18] developed a curvature-driven computational model to capture neotissue growth kinetics across scaffold pores of increased complexity able to simulate up until complete infilling of all the pores (Fig. 4.2).

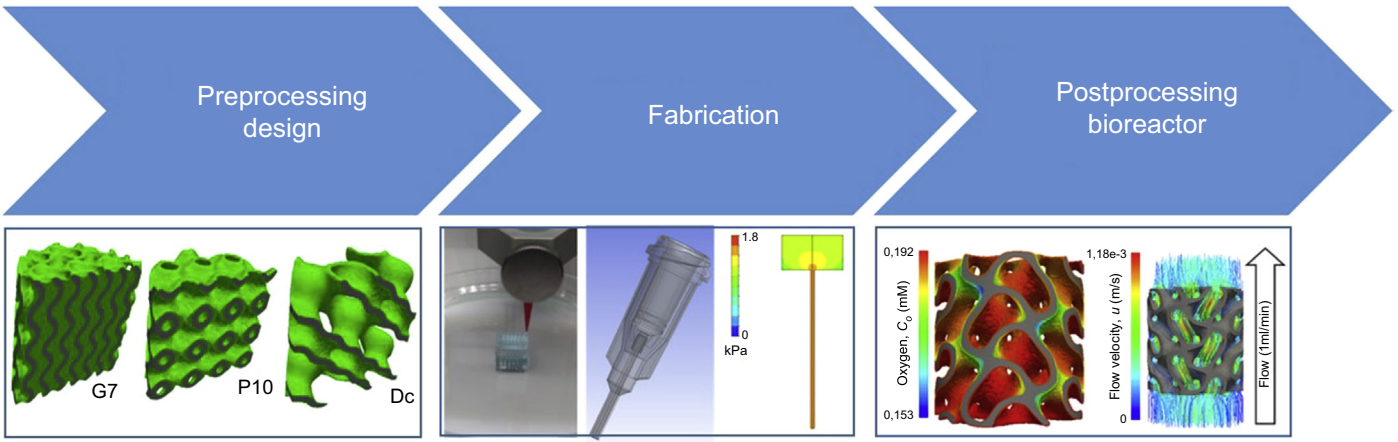

Figure 4.1 Schematic overview of this chapter, illustrating the different steps discussed in the text. (1) Preprocessing: design of scaffold geometries [4]. (2) Fabrication: simulation of mechanical environment during 3D extrusion-based bioprinting (unpublished). (3) Postprocessing: bioreactor culture showing quantification of local oxygen concentration and fluid flow velocity [5].

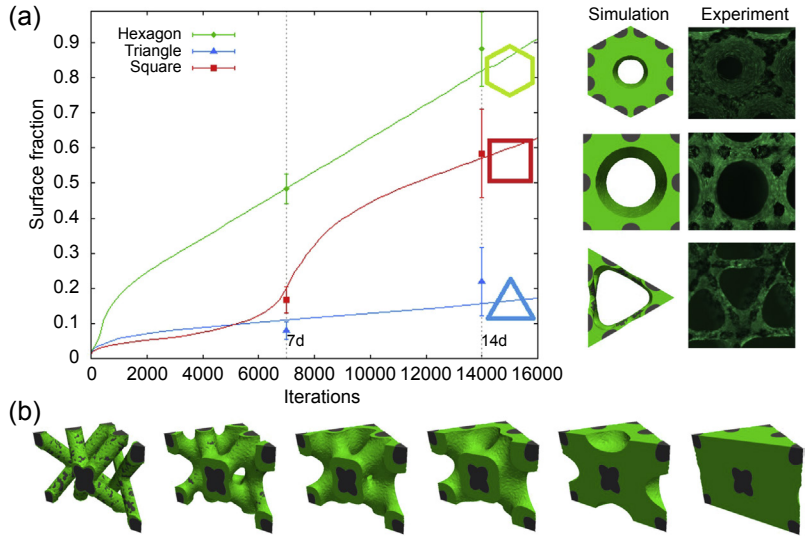

Figure 4.2 Curvature-driven neotissue (cell + the ECM they produce) growth dynamics in complex 3D scaffolds. (a) Simulation of neotissue growth in 3D-printed titanium scaffolds with three different unit cell geometries (triangle, square, hexagon). Calibration with experimental findings by comparing surface fraction of the unit cell in simulations and experiments. Calibration point used is hexagon (iteration 7000 = 7 days in culture). Right: visual comparison of obtained neotissue geometry (left) and experimentally observed neotissue formation (right). (b) Simulation of complex diamond-shaped unit cell, demonstrating the capacity of the in silico model to simulate neotissue growth up to complete filling.
Adapted with permission from Springer from Y. Guyot, I. Papantoniou, Y.C. Chai, S. Van Bael, J. Schrooten, L. Geris, A computational model for cell/ECM growth on 3D surfaces using the level set method: a bone tissue engineering case study, Biomech Model Mechanobiol 13 (6) (November 2014) 1361–1371, https://doi.org/10.1007/s10237-014-0577-5. Epub 2014 Apr 3.

4.2.2 Mechanical properties

A major role of scaffolds is to provide structural support to the cultured cells while tissues are engineered in vitro. In addition, scaffold stiffness regulates tissue regeneration upon implantation. Therefore, the mechanical properties of the produced scaffolds have long been a focus of computational investigation (cf. the aforementioned work by Hollister, Fernandes et al.). When assessing whole-implant scale scaffolds, computational models can define mechanical properties that will be comparable with those encountered at the implantation site aiding incorporation and host integration [19,20]. Additionally, the mechanical loading encountered after implantation can be coupled, for instance, to vascular development with bone tissue formation [21].

Fluid–structure interaction (FSI) approaches have been applied to understand the role of scaffold stiffness and architecture on the wall shear stress distribution. In fact, McCoy [22] determined that the applied flow rate dominated the mechanical stimulation when compared with the pore size in collagen–GAG scaffolds. More recently, Zhao et al. [23] applied this method to investigate the role of scaffold geometry

(architecture, pore size, and porosity) on pore wall shear stress (WSS) under a range of different loading scenarios (being fluid perfusion, mechanical compression, and a combination of perfusion and compression), finding that scaffold geometry (spherical and cubical pores), and in particular the pore size, has a significant influence on the stimulation within the scaffolds. In addition, they concluded that the combination of loading conditions would allow amplifying these wall shear stresses. Fluid–structure interaction has been used to simulate how the fluid movement deforms the cell body, modeling the cell as a solid in many different applications of tissue engineering. Vaughan [24] developed a fluid–structure interaction model to characterize the deformation of integrin and primary cilia-based mechanosensors in bone cells under fluid flow stimulation. Recently, immersed boundary models were used to quantify compressive and shear stresses developed over deformable virtual cells of various shapes and scaffold locations when exposed in fluidic environment [5].

4.2.3 Modeling scaffold degradability

The ability to quantitatively decipher physical, chemical, and biological phenomena involved in the controlled release of ions or molecules [25,26] requires the use of in silico models. Concerning the development of optimized degradable scaffolds, the importance of such models lies in their relevance during the designing stage as well as the experimental verification of degradation and release mechanism(s). However, it is unlikely that there will be one single in silico model that will be able to describe any type of release of ions or molecules from biomaterials. Scaffold degradation should give way gradually to new native tissue, leading to complete scaffold disappearance. Scaffold degradation usually takes place by chemical pathways (hydrolysis) in the case of polymeric scaffolds and has been a focus of numerical analysis studies by, e.g., Adachi et al. [7,27]. Thorough understanding of hydrolysis kinetics can control the rate of scaffold mass loss, enabling the design of polymer biomaterials for tailored applications. Pioneering studies on species (drug) release from scaffold–polymer systems has been extensively carried out [25,28]. However, given the particularities of bioprinting and tissue engineering, this domain is still not adequately studied.

Over the past few years, a few lattice-based three-dimensional (3D) in silico models have been proposed to study the in vivo bone formation process in porous biodegradable CaP scaffolds [29,30]. Byrne et al. [29] developed an in silico model of in vivo tissue differentiation and bone regeneration in a degrading scaffold as a function of porosity, Young's modulus, and dissolution rate. Sun et al. [30] proposed a multiscale model of a biodegradable porous calcium phosphate (CaP) scaffold to examine the effects of pore size and porosity on bone formation and angiogenesis. However, the aforementioned models did not capture the actual geometry of the degrading CaP scaffolds, which was demonstrated by Manhas et al. [31]. Lastly, a series of investigations reported on the development of in silico models for bioglass scaffolds and their degradation properties for bone tissue engineering [32], whereas agent-based models were used to capture degradation in function to invading vascularization [33]. Even more intricate models capturing geometric complexities such as the design of biodegradable interbody fusion cages have been recently carried out [34]. These models

had phenomenological description of the degradation process and were interested in the degradation products themselves but also in the changing stiffness and porosity of the scaffold.

4.2.4 Mass transport

Before the printing process, the performance of implants can already be verified by simulating the transport of oxygen, nutrients, and waste products in the printed materials. Shipley et al. [35] investigated the design of an extrusion-based printed construct (gel + cells) in terms of printed geometrical configuration (strand thickness and density) and speed of perfusion of medium throughout the construct in a perfusion bioreactor system.

Besides transport of nutrients and waste products, also other transport can be simulated. For example, Carlier et al. [36] demonstrated using a previously established computational model of bone regeneration [37,38], spatially patterned constructs enhance bone regeneration compared with constructs with a uniform cell distribution. The model accounts for cells, their extracellular matrix as well as the presence (and diffusion) of growth factors. The models allow testing the printing pattern of complex implants before printing during the design process in bioprinting.

4.3 The fabrication process

Scaffolds have been fabricated using various fabrication methodologies ranging from decellularization techniques to the use of additive manufacturing as discussed in Chapter 6 in this volume [113]. The choice of the production process determines the range of materials that can be used and the scaffold design characteristics that can be fabricated. Moreover, when materials and cells are combined in the same fabrication process, as is the case in the field of bioprinting, an extra level of complexity is added to the design of the production process to obtain a viable construct with the desired scaffold properties. To ensure that the fabricated scaffolds meet the requirements linked to architecture and biocompatibility, the production process should be well designed and robust. In conventional fabrication methods, the degree of control over the micro- and nanostructure is limited and therefore difficult to predict. Although additive manufacturing techniques allow for a precise spatiotemporal material deposition, the shape fidelity is often decreased by the fabrication process. Optimization is needed but challenging and tedious because of the multifactorial nature of the process, and a trial-and-error approach is currently mostly used in which one parameter is changed and the effect of the change is investigated experimentally [39–41]. To overcome these hurdles, computational modeling can offer an important tool that allows for a more efficient screening of the influence of process parameters on the robustness of the fabrication process and the quality of the outcome. In the following paragraphs, a few examples are given of how computational modeling can play a role in the design of the fabrication process.

4.3.1 Shape fidelity in function of the fabrication process

The theoretical design of a scaffold often differs from the actual architecture because of the influence of the fabrication process on parameters such as layer height and wall thickness, thereby reducing the shape fidelity of the actual object. Although great advances in scaffold design have been obtained by using computational modeling for optimizing the scaffold's topology, surface, and size, models describing how the fabrication process influences these parameters are still scarce. Castilho et al. suggested that it might be considered to add a correction factor to the computational model describing the design of the scaffold to correct for the observed deviations introduced by the setup of the printing process [42].

In an attempt to predict the shape of a printed object taking into account the effect of its printing process, Suntornnond et al. developed an in silico model that describes the resolution of the printed width of a continuous hydrogel line as a function of nozzle size, pressure, and printing speed [43].

In addition, the behavior of materials during printing is dependent on their rheological profile and the design of the printing setup. Recently, a model has been proposed to describe the printability of inks in function of the design of the needles used in a pressure-driven, shear-thinning, extrusion-based printing process [44], and the influence of different printing parameters on viscoelastic stresses within the inks and print fidelity has been simulated in a computational fluid dynamics analysis [45]. To analyze the shape of the hydrogel extruded, Lee and Yeong [46] developed a model for a time–pressure extrusion-based biodispensing system (Fig. 4.3).

4.3.2 Biocompatibility of the fabrication process conditions

In bioprinting strategies, it is key to understand, characterize, and select the optimal process parameters needed to produce a cell-based construct that guides tissue development. These parameters will depend on the fabrication technology and the formulation of the bioinks used. The ideal bioink process interplay should ensure printability and biocompatibility at all phases of the bioprinting process and should lead to mechanical integrity and structural stability of the construct [47,110].

Different additive manufacturing technologies exist to fabricate scaffolds or cell-based constructs, and each setup has its own properties that can influence the production process as discussed in other chapters. Several computational models have been developed to gain insight in how the printed object is affected by the specific system specifications and help in determining the window in which the bioinks are printable and ensure cell survival (Fig. 4.2). Evaluating the flow forces acting onto cell–material mixtures for different setups, for instance, is difficult to observe with biological analyses only and requires a description of the physics related to the fabrication process to quantify said forces. Numerical techniques have the potential to predict and mimic the mechanochemical microenvironments of cells during the bioprinting process under various protocols as well as to optimize process parameters. Both classical theoretical calculations and finite element analyses may be applied. Through these in silico models, more insights can be obtained into construct properties at the different steps of the bioprinting process [2].

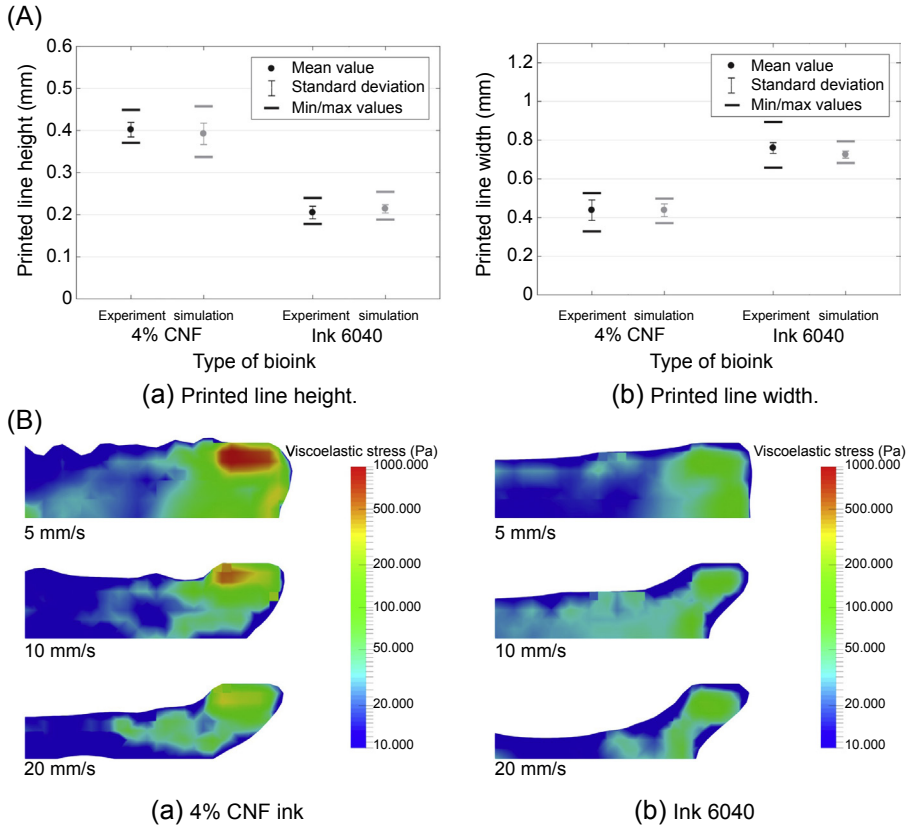

Figure 4.3 Predicting bioprintability of nanofibrillar inks using computer simulations of the 3D bioprinting process. (A) Comparison of experimental observations and model simulations for printed line height (a) and printed line width (b) for two different nanofibrillar bioinks. (B) Simulated distribution of viscoelastic stresses in the printed ink incurred during the printing process for two different nanofibrillar bioinks.
Adapted from J. Gohl, et al., Simulations of 3D bioprinting: predicting bioprintability of nanofibrillar inks, Biofabrication 10 (3) (2018) 034105 under the CC BY license.

To predict the shape of the scaffold and cell survival in *inkjet printing*, it is important to understand the droplet ejection in thermal inkjet printheads [48]. Pepper et al. modeled, both analytically and by means of FE methods, the cell settling effects in inkjet printing [49,50]. Tirella et al. used a finite element model to investigate the role of the stiffness of the deposition substrate during droplet impact during inkjet printing process [51]. For *laser-induced forward transfer* (LIFT) printing, Mezel [52] presented a 2D axisymmetric model to analyze jet formation. This analysis contributes to the understanding of the ejection process and aims to reduce the biological damage during printing.

In *extrusion-based bioprinting*, the compromise between printability and biocompatibility may be achieved by manipulating the temperature, the geometry of the dispensing setups, the dispensing pressure, shear stress, and the bioink concentration

among others [53]. The flow rate has a direct effect on the pore size and porosity of the scaffolds formed and therefore on its mechanical and biological properties. To analyze the effect of the nozzle geometry on the flow rate, non-Newtonian flow is considered. The flow rate in a cylindrical needle can be expressed as:

$$Q = \frac{\pi R^3 n}{1+3n}\left[\frac{\Delta PR}{2KL}\right]^{1/n} \tag{4.1}$$

where R and L are the nozzle length and radius, K is the consistency index, the constant n is the power law index, and ΔP is the pressure drop in the needle. The flow rate in a tapered needle is given by [54]:

$$Q = \frac{\pi D_i^3 D_o^3}{32}\left[\frac{3n\,\Delta P\,(D_i - D_o)}{4KL\left(D_i^{3n} - D_o^{3n}\right)}\right]^{1/n} \tag{4.2}$$

where D_i and D_o are the entrance and exit diameters of the tapered nozzle, respectively. Therefore, according to these equations, the flow rates in the tapered nozzles are much higher under the same pressure conditions, owing to the smaller diameter size at the exit.

During the extrusion-based bioprinting process, cells are subjected to shear stresses. It is well known that higher shear stresses lead to lower cell viability [53,55]. Blaeser et al. [56] found that shear stress should be controlled within 5 kPa to obtain more than 90% living cells for mouse fibroblasts in a valve-based jet printing process. In fact, the percentage of cell damage (I) may be directly related to the shear stress cell experience (τ) through the very simple and well-established power law [57,58].

$$I(\%) = Ct^a\tau^b \tag{4.3}$$

where t is the exposure time. C, a, and b are constants for a given type of cells. To reduce cell damage due to shear stress, instead of directly printing cells loaded within the biomaterial, they may be encapsulated in spheroids [59].

The level of shear stress is directly related to different bioprinting parameters, such as viscosity of the bioink, pressure, or nozzle geometry [55,56]. The shear stress is related to the viscosity (μ) through the shear rate ($\dot{\gamma}$):

$$\tau = \mu\dot{\gamma} = K\dot{\gamma}^n \tag{4.4}$$

where K is the consistency index and the constant n is the power law index. A sudden decrease of shear rates during deposition may cause an increase in viscosity, resulting in a high printing fidelity and higher cell viability. The relationship between the maximum shear stress in the wall and pressure drop is given by Ref. [55]:

$$\tau_{max} = \left(\frac{n}{3n+1}\right)^n \frac{D}{4}\Delta P \tag{4.5}$$

where D is the nozzle diameter. In addition, the shear stresses increase with the nozzle radius, from zero at the needle center to its maximum value in the wall. Thus, at equivalent flow rates, shear stress and consequently cell damage in a tapered needle is lower than in a cylindrical one owing to its lower value of exit radius. This has been already analyzed both in vivo and in silico [54].

To favor cell survival in extrusion-based bioprinting, the dispensing pressure must be maintained as low as possible. A higher dispensing pressure can allow ejecting highly viscous bioinks, but this could increase the shear stress, which reduces cell viability (Eq. 4.3). Billiet et al. [53] have compared cell viabilities under different dispensing pressures and needle geometries. They found that at low inlet pressures (high passage time), tapered needles are preferred over cylindrical ones. At high inlet pressure (low passage time), substantially higher shear stresses are induced and a higher viability level is observed for the cylindrical type. Nair et al. [55] characterized the viability of endothelial cells during extrusion-based printing, and the results indicated that dispensing pressure had a more significant effect on cell viability than the nozzle diameter. However, under the same pressure conditions, the level of force cells experienced in tapered nozzles is much higher than in cylindrical nozzles owing to its much larger surface at the entrance (pressure = force/area). This may cause cells to be harmed and even die.

4.3.3 Biological functionality after the fabrication process

After cell printing, three possible outcomes may occur: (1) cell survival with desired phenotype, (2) cell survival but cells become quiescent and they may recover and differentiate into diverse specialized cell types or die; and (3) immediate necrosis due to high shear stress, clotting in the nozzle or no tissue printed. Computer models can help to assess whether tissues are able to function as intended after the fabrication process. For the particular case of extrusion bioprinting, complex in silico modeling via cellular particle dynamics (CPD) simulations can be used to predict postprinting structure formation even in the case of volume changing bioink units [60,61]. A method based on kinetic Monte Carlo simulations has also been used to describe the shape evolution of multicellular systems postbioprinting [62–69]. Yang et al. [70] studied the morphological development of the printed bioconstructs during fusion by means of an in silico model based on the phase field formulation.

4.4 Postprocessing: bioreactor culture

To deal with the increasing mass transport requirements of growing engineered tissues in vitro, the majority of scaffolds will need to be coupled to bioreactor systems for stem cell growth and differentiation. This requires the use of in silico models of higher complexity to decipher the increased complexity posed by this interplay between the dynamic culture environment and scaffold properties [71].

4.4.1 Incorporating the neotissue domain

Initially, computational fluid dynamics (CFD) simulations were developed and used to characterize flow patterns in (mostly empty) scaffolds to quantify the local flow-induced shear stresses acting on the attached cells [72–76]. For scaffolds with ordered pores structures, Truscello et al. [77] showed that the permeability can be defined accurately through CFD approaches. These computational studies supported initial experimental tissue engineering studies where cells were attached on scaffold struts and wall shear stresses experienced by the cells were important in determining their differentiation [22,78–80]. However, during culture, cells and the extracellular matrix they produce (together indicated with the term "neotissue") eventually fill the scaffold (as characterized, for instance, in Ref. [81]), which will significantly affect the flow profile. This means that modeling empty scaffolds is inadequate for the determination of the true mechanical environment that seeded cells will experience over culture time. Initial efforts to address incorporate neotissue growth were undertaken; however, the neotissue volume was modeled as an impermeable structure leading to overestimated surface shear stresses [82,90]. Because the neotissue is a permeable structure permitting flow even at complete filling of the scaffold [83], it is important to consider the fluid velocity field developed within the neotissue to correctly determine the gradients developed within it. More recent studies have managed to carry out CFD analysis, while neotissue growth is occurred by using the level set method coupled to the Brinkman equation [84]. In addition, the neotissue growth kinetics were also coupled to shear stresses experienced by the cells, which were influenced in a dose-dependent manner [85]. Along these lines, Williams et al. used a lattice Boltzman model for quantifying the fluid dynamics in their system and they were able to monitor time-dependent mineralization of neotissue during growth [86].

4.4.2 Multiphysics models for scaffolds in bioreactors

Deciphering the microenvironment that defines stem cell survival and fate is a daunting task because a multitude of factors need to be quantified instantaneously. To date, very few experimental studies report on important environmental cues such as dissolved oxygen tension, glucose, lactate, and pH all impacting stem cell state and neotissue properties. For instance, very low glucose and oxygen concentrations in the system could lead to cell death, whereas an important amount of lactate will decrease the medium pH and inhibit cell proliferation capacity [87]. In addition, pH can play a crucial role in bone tissue engineering applications as human MSC osteogenic differentiation has been seen to be inhibited in specific pH ranges [88]. Despite the importance of these physicochemical factors on the outcome of the bioreactor process, their local quantification in growing neotissues (through, e.g., sensors) remains problematic, thereby severely limiting the product quality control and the translation to clinical practice. Limited computational studies have attempted to model the (multiparametric) physicochemical environment experienced by growing cells within a bioreactor setup (for instance, [89–91] and [4]). In those studies, the authors introduced oxygen, glucose, and lactate with the help of diffusion–convection–reaction equations

to determine the local concentration of these metabolic species in the context of bioreactor processes geared toward in vitro cartilage or neotissue growth. In addition, a model for coupling mechanical properties of struts and mass transport was also recently published [8]. However, certain limitations were present in terms of confluence levels that the growing domain could reach as well as in terms of the global (length) scale that could be modeled. This is a broad field where computational studies are required for mapping dynamic and time evolving biological systems from the niche to the whole-implant scale.

4.5 Discussion

4.5.1 Multiparametric optimization

The determination of the optimal combination of the aforementioned scaffold and process properties is a daunting task. It is difficult to define what constitutes an optimal solution to a problem as there may be multiple, conflicting objectives. Hence the use of multiobjective optimization methods (MOOs) can allow to identify optimal trade-off between "costs" (e.g., cost of materials, time, and negative side effects) and "rewards" (e.g., successful neotissue growth). Furthermore, design of experiments (DoE) is an essential tool for quality by design (QbD) that allows the systematic and parallel investigation of multiple process parameters on scaffold properties and printed cell characteristics. By using this method, a ranking of the process parameters is achieved in terms of the most influential parameters in light of the target output panel. This method takes into account the interaction of parameter interrelationship, using linear regression and analysis of variance (ANOVA) in silico models [92]. Recent work by Ruiter, Nazir, Desai, and their respective coworkers focused on finding optimal electrospinning process parameters (polymer composition, dispensing distance, voltage, and flow rate), which significantly influenced the fiber diameter, morphologies, and bead distribution observed in electrospinning of poly-D-L-lactic acid (PDLLA) fibers [93–95]. Similarly, few DoE studies exist for melt extrusion bioprinting where temperature, pressure, and nozzle diameter have been optimized for scaffold compression strength [96]. Ravi et al. designed a modular 3D printing setup combining different fabrication technologies and they used a DoE to characterize the setup and to assess the relation between fabrication process parameters and their effect on printed scaffold characteristics [97]. For scaffolds cultured in bioreactors, DoEs have been used to investigate optimal seeding density and fluid flow to produce scaffolds with optimal presence of neotissue [80].

As the multivariable complexity of new processes and materials increases, the task of identifying the best combination of process settings to achieve output material property targets becomes complex and time-consuming and DoE still requires considerable experimentation. High-throughput experimental setups can be developed to assess certain aspects of scaffold (printer) design such as the case for surface topography in the TopoChip setup [111]. These data sets need to be handled using appropriate algorithms from the big data and -omics domain. Alternatively, advanced optimization methods capable of making better use of less data are required. Topological

optimization algorithms have been recently published [98] together with mechanobiology-driven algorithms for bone tissue engineering applications [99]. Relevant black-box (i.e., data-driven or empirical) optimization methods include genetic algorithms, trust-region methods, and Bayesian optimization [100–104]. Black-box methods give flexibility with respect to the black-box contents. If there are no restrictions on the black box, the optimization methods are equally relevant to in vitro experiments as legacy computer code. MOO methods explicitly find the trade-offs between conflicting objectives [105–107].

4.5.2 Future prospects

In silico models are increasingly present in the life cycle of medicinal products, not only in the design phase but also in the development phase, the clinical trial phase as well as for postmarketing surveillance purposes. To build model credibility, the so-called VVUQ (verification–validation–uncertainty quantification) needs to be established. Verification answers the question whether the computed results correspond to the mathematical equations. Validation answers the questions whether the computed results correspond to physical reality. This needs to be complemented with uncertainty quantification, in which the effect of the uncertainties in the model assumptions and parameters on the simulation outcome is determined. For medical devices, reporting guidelines have been established by the FDA for inclusion of in silico evidence in regulatory dossiers (https://www.fda.gov/downloads/MedicalDevices/DeviceRegulationandGuidance/GuidanceDocuments/UCM381813.pdf). Furthermore, in collaboration with industry and academia, a clear procedure has been established to perform verification and validation of the developed in silico models that are (part of) a medical device or have delivered digital evidence that was important in the R&D process of a medical device presented in a regulatory dossier [108,109]. Currently, ASME and its partners are also working on a VVUQ standard specifically dedicated to advanced (including additive) manufacturing (https://cstools.asme.org/csconnect/CommitteePages.cfm?Committee=101978604). These focus on development of standards in a clear sign of maturity of the in silico technology. Adding the biological aspects into the models moves the application from a medical device toward an advanced therapeutic medicinal product (ATMP), which brings along additional challenges in terms of model establishment and validation. Nevertheless, given the recent advances in fabrication technologies and the increasing demands on the complexity of the applications, computational models will become indispensable for rational production of tissue-engineered implants.

Acknowledgments

Research was funded by the Research Foundation Flanders (FWO Vlaanderen; I.P: 12O7916N), the Fund for National Research (FNRS; T.0256.16), and the European Research Council under the European Union's Horizon 2020 framework program ERC/CoG 772418 (L.G.). This work is supported by Regenerative Medicine Crossing Borders (www.regmedxb.com), powered by EWI-Vlaanderen.

The funders had no role in study design, data collection and analysis, decision to publish, or preparation of the manuscript. This work is part of Prometheus, the KU Leuven R&D division for skeletal tissue engineering (http://www.kuleuven.be/prometheus).

References

[1] A.B. Dababneh, I.T. Ozbolat, Bioprinting technology: a current state-of-the-art review, J Manuf Sci Eng 136 (6) (2014) 061016.
[2] C. Mandrycky, Z. Wang, K. Kim, D.H. Kim, 3D bioprinting for engineering complex tissues, Biotechnol Adv 34 (4) (2016) 422–434.
[3] S.V. Murphy, A. Atala, 3D bioprinting of tissues and organs, Nat Biotechnol 32 (8) (2014) 773–785.
[4] Y. Guyot, A Multiphysics Multiscale Computational Framework for the Simulation of Perfusion Bioreactor Processes in Bone Tissue Engineering, 2015 (Ph.D. dissertation). http://hdl.handle.net/2268/189105.
[5] Y. Guyot, B. Smeets, T. Odenthal, R. Subramani, F.P. Luyten, H. Ramon, et al., Immersed boundary models for quantifying flow-induced mechanical stimuli on stem cells seeded on 3D scaffolds in perfusion bioreactors, PLoS Comput Biol 12 (9) (2016) e1005108. https://doi.org/10.1371/journal.pcbi.1005108.
[6] M.A. Alias, P.R. Buenzli, Modelling the effect of curvature on the collective behavior of cells growing new tissue, Biophys J 112 (1) (2017) 193–204.
[7] T. Adachi, Y. Osako, M. Tanaka, M. Hojo, S.J. Hollister, Framework for optimal design of porous scaffold microstructure by computational simulation of bone regeneration, Biomaterials 27 (2006) 3964–3972. 16584771.
[8] M.R. Dias, J.M. Guedes, C.L. Flanagan, S.J. Hollister, P.R. Fernandes, Optimization of scaffold design for bone tissue engineering: a computational and experimental study, Med Eng Phys 36 (4) (2014) 448–457.
[9] S.J. Hollister, R.D. Maddox, J.M. Taboas, Optimal design and fabrication of scaffolds to mimic tissue properties and satisfy biological constraints, Biomaterials 23 (2002) 4095–4103, https://doi.org/10.1016/S0142-9612(02)00148-5.
[10] H.C. Rodrigues, P.G. Coelho, P.R. Fernandes, Multiscale modelling of bone tissue – remodelling and application to scaffold design, in: in: P. Fernandes, P. Bártolo (Eds.), Advances on Modelling in Tissue Engineering. Computational Methods in Applied Sciences, vol. 20, Springer, Dordrecht, 2011.
[11] J.M. Taboas, R.D. Maddox, P.H. Krebsbach, S.J. Hollister, Indirect solid free form fabrication of local and global porous, biomimetic and composite 3D polymer–ceramic scaffolds, Biomaterials 24 (2003) 181–194, https://doi.org/10.1016/S0142-9612(02)00276-4.
[12] J.A. Sanz-Herrera, J.M. García-Aznar, M. Doblaré, On scaffold designing for bone regeneration: a computational multiscale approach, Acta Biomater 5 (2009) 219–229.
[13] S. Van Bael, Y.C. Chai, S. Truscello, M. Moesen, G. Kerckhofs, H. Van Oosterwyck, J. Schrooten, The effect of pore geometry on the in vitro biological behavior of human periosteum-derived cells seeded on selective laser-melted Ti6Al4V bone scaffolds, Acta Biomater 8 (7) (2012) 2824–2834.
[14] M. Werner, S.B.G. Blanquer, S.P. Haimi, G. Korus, J.W.C. Dunlop, G.N. Duda, D.W. Grijpma, A. Petersen, Adv Sci 4 (2017) 1600347.
[15] M.A. Alias, P.R. Buenzli, Osteoblasts infill irregular pores under curvature and porosity controls: a hypothesis-testing analysis of cell behaviours, Biomech Model Mechanobiol 17 (5) (2018) 1357–1371.

[16] C.M. Bidan, K.P. Kommareddy, M. Rumpler, P. Kollmannsberger, Y.J.M. Bréchet, P. Fratzl, et al., How linear tension converts to curvature: geometric control of bone tissue growth, PLoS One 7 (5) (2012) e36336. https://doi.org/10.1371/journal.pone.0036336.
[17] C.M. Bidan, P. Kollmannsberger, V. Gering, S. Ehrig, P. Joly, A. Petersen, V. Vogel, P. Fratzl, J.W. Dunlop, Gradual conversion of cellular stress patterns into pre-stressed matrix architecture during in vitro tissue growth, J R Soc Interface 13 (118) (2016) 20160136.
[18] Y. Guyot, I. Papantoniou, Y.C. Chai, S. Van Bael, J. Schrooten, L. Geris, A computational model for cell/ECM growth on 3D surfaces using the level set method: a bone tissue engineering case study, Biomech Model Mechanobiol 13 (6) (November 2014) 1361–1371, https://doi.org/10.1007/s10237-014-0577-5. Epub 2014 Apr 3.
[19] L. Grassi, S.P. Vaananen, S. Amin Yavari, H. Weinans, J.S. Jurvelin, A.A. Zadpoor, H. Isaksson, Experimental validation of finite element model for proximal composite femur using optical measurements, J Mech Behav Biomed Mater 21 (2013) 86–94, https://doi.org/10.1016/j.jmbbm.2013.02.006.
[20] S.-I. Roohani-Esfahani, P. Newman, H. Zreiqat, Design and fabrication of 3D printed scaffolds with a mechanical strength comparable to cortical bone to repair large bone defects, Sci Rep 6 (2016) Article number: 19468.
[21] S. Checa, P.J. Prendergast, A mechanobiological model for tissue differentiation that includes angiogenesis: a lattice-based modelling approach, Ann Biomed Eng 37 (1) (2009) 129–145.
[22] R.J. McCoy, C. Jungreuthmayer, F.J. O-Brien, Influence of flow rate and scaffold pore size on cell behavior during mechanical stimulation in a flow perfusion bioreactor, Biotechnol Bioeng 109 (2012) 1583–1594.
[23] F. Zhao, T.J. Vaughan, L.M. McNamara, Quantification of fluid shear stress in bone tissue engineering scaffolds with spherical and cubical pore architectures, Biomech Model Mechanobiol 15 (3) (2016) 561–577.
[24] T.J. Vaughan, C.A. Mullen, S.W. Verbruggen, L.M. McNamara, Bone cell mechanosensation of fluid flow stimulation: a fluid-structure interaction model characterising the role integrin attachments and primary cilia, Biomech Model Mechanobiol 14 (4) (2015) 703–718.
[25] J. Siepmann, H. Kranz, R. Bodmeier, N. Peppas, HPMC-matrices for controlled drug delivery: a new model combining diffusion, swelling, and dissolution mechanisms and predicting the release kinetics, Pharm Res 16 (1999) 1748–1756.
[26] B.S. Snorradóttir, F. Jónsdóttir, S.T. Sigurdsson, F. Thorsteinsson, M. Másson, Numerical modelling and experimental investigation of drug release from layered silicone matrix systems, Eur J Pharm Sci 49 (2013) 671–678.
[27] Y. Wang, J. Pan, X. Han, C. Sinka, L. Ding, A phenomenological model for the degradation of biodegradable polymers, Biomaterials 29 (2008) 3393–3401.
[28] C.S. Brazel, N.A. Peppas, Modelling of drug release from swellable polymers, Eur J Pharm Biopharm 49 (2000) 47–58.
[29] D.P. Byrne, D. Lacroix, J.A. Planell, D.J. Kelly, P.J. Prendergast, Simulation of tissue differentiation in a scaffold as a function of porosity. Young's modulus and dissolution rate: application of mechanobiological models in tissue engineering, Biomaterials 28 (2007) 5544–5554.
[30] X. Sun, Y. Kang, J. Bao, Y. Zhang, Y. Yang, X. Zhou, Modelling vascularized bone regeneration within a porous biodegradable CaP scaffold loaded with growth factors, Biomaterials 34 (2013) 4971–4981.
[31] V. Manhas, Y. Guyot, G. Kerckhofs, Y.C. Chai, L. Geris, Computational modelling of local calcium ions release from calcium phosphate-based scaffolds, Biomech Model Mechanobiol 16 (2017) 425. https://doi.org/10.1007/s10237-016-0827-9.

[32] J.A. Sanz-Herrera, A.R. Boccaccini, Modelling bioactivity and degradation of bioactive glass based tissue engineering scaffolds, Int J Solid Struct 48 (2) (2011) 257–268.
[33] H. Mehdizadeh, E.S. Bayrak, C. Lu, S.I. Somo, B. Akar, E.M. Brey, A. Cinar, Agent-based modeling of porous scaffold degradation and vascularization: optimal scaffold design based on architecture and degradation dynamics, Acta Biomater 27 (November 2015) 167–178, https://doi.org/10.1016/j.actbio.2015.09.011. Epub 2015 Sep. 9.
[34] H. Kang, S.J. Hollister, F. La Marca, P. Park, C.-Y. Lin, Porous biodegradable lumbar interbody fusion cage design and fabrication using integrated global-local topology optimization with laser sintering, J Biomech Eng 135 (2013) 101013. 23897113.
[35] R.J. Shipley, G.W. Jones, R.J. Dyson, B.G. Sengers, C.L. Bailey, C.P. Please, J. Malda, Design criteria for a printed tissue engineering construct: a mathematical homogenization approach, J Theor Biol 259 (2) (2009) 489–502, https://doi.org/10.1016/j.jtbi.2009.03.037.
[36] A. Carlier, G.A. Skvortsov, F. Hafezi, E. Ferraris, J. Patterson, B. Koç, H. Van Oosterwyck, Computational model-informed design and bioprinting of cell-patterned constructs for bone tissue engineering, Biofabrication 8 (2) (May 17, 2016) 025009, https://doi.org/10.1088/1758-5090/8/2/025009.
[37] A. Carlier, L. Geris, N. van Gastel, G. Carmeliet, H. Van Oosterwyck, Oxygen as a critical determinant of bone fracture healing-a multiscale model, J Theor Biol 365 (January 21, 2015) 247–264, https://doi.org/10.1016/j.jtbi.2014.10.012. Epub 2014 Oct 24.
[38] A. Carlier, L. Geris, K. Bentley, G. Carmeliet, P. Carmeliet, H. Van Oosterwyck, MOSAIC: a multiscale model of osteogenesis and sprouting angiogenesis with lateral inhibition of endothelial cells, PLoS Comput Biol 8 (10) (2012) e1002724, https://doi.org/10.1371/journal.pcbi.1002724.
[39] A. Farzadi, et al., Effect of layer thickness and printing orientation on mechanical properties and dimensional accuracy of 3D printed porous samples for bone tissue engineering, PLoS One 9 (9) (2014) e108252.
[40] T. Gao, et al., Optimization of gelatin-alginate composite bioink printability using rheological parameters: a systematic approach, Biofabrication 10 (3) (2018) 034106.
[41] M. Perez, et al., Surface quality enhancement of fused deposition modelling (FDM) printed samples based on the selection of critical printing parameters, Materials 11 (8) (2018).
[42] M. Castilho, M. Dias, U. Gbureck, J. Groll, P. Fernandes, I. Pires, B. Gouveia, J. Rodrigues, E. Vorndran, Fabrication of computationally designed scaffolds by low temperature 3D printing, Biofabrication 5 (3) (September 2013) 035012, https://doi.org/10.1088/1758-5082/5/3/035012.
[43] R. Suntornnond, et al., A mathematical model on the resolution of extrusion bioprinting for the development of new bioinks, Materials 9 (9) (2016).
[44] N. Paxton, et al., Proposal to assess printability of bioinks for extrusion-based bioprinting and evaluation of rheological properties governing bioprintability, Biofabrication 9 (4) (2017) 044107.
[45] J. Gohl, et al., Simulations of 3D bioprinting: predicting bioprintability of nanofibrillar inks, Biofabrication 10 (3) (2018) 034105.
[46] J.M. Lee, W.Y. Yeong, A preliminary model of time-pressure dispensing system for bioprinting based on printing and material parameters, J Virtual Phys Prototyp 10 (2015) 3–8.
[47] D. Chimene, et al., Advanced bioinks for 3D printing: a materials science perspective, Ann Biomed Eng 44 (6) (2016) 2090–2102.
[48] H. Tan, et al., Numerical simulation of droplet ejection of thermal inkjet printheads, Int J Numer Methods Fluid 77 (2015) 544–570.

[49] M.E. Pepper, V. Seshadri, T. Burg, B.W. Booth, K.J. Burg, R.E. Groff, Cell settling effects on a thermal inkjet bioprinter, Conf Proc IEEE Eng Med Biol Soc 2011 (2011) 3609–3612, https://doi.org/10.1109/IEMBS.2011.6090605.
[50] M.E. Pepper, V. Seshadri, T.C. Burg, K.J. Burg, R.E. Groff, Characterizing the effects of cell settling on bioprinter output, Biofabrication 4 (1) (March 2012) 011001, https://doi.org/10.1088/1758-5082/4/1/011001. Epub 2012 Jan 18.
[51] A. Tirella, F. Vozzi, C. De Maria, G. Vozzi, T. Sandri, D. Sassano, L. Cognolato, A. Ahluwalia, Substrate stiffness influences high resolution printing of living cells with an ink-jet system, J Biosci Bioeng 112 (1) (July 2011) 79–85, https://doi.org/10.1016/j.jbiosc.2011.03.019.
[52] C. Mezel, et al., Bioprinting by laser-induced forward transfer for tissue engineering applications: jet formation modelling, Biofabrication 2 (1) (2010) 014103.
[53] T. Billiet, E. Gevaert, T. De Schryver, M. Cornelissen, P. Dubruel, The 3D printing of gelatin methacrylamide cell-laden tissue-engineered constructs with high cell viability, Biomaterials 35 (2014) 49–62.
[54] M. Li, X. Tian, D.J. Schreyer, X. Chen, Effect of needle geometry on flow rate and cell damage in the dispensing-based biofabrication process, Biotechnol Prog 27 (2011) 1777–1784.
[55] K. Nair, M. Gandhi, S. Khalil, K.C. Yan, M. Marcolongo, K. Barbee, W. Sun, Characterization of cell viability during bioprinting processes, Biotechnol J 4 (2009) 1168–1177.
[56] A. Blaeser, D.F.D. Campos, U. Puster, W. Richtering, M.M. Stevens, H. Fischer, Controlling shear stress in 3D bioprinting is a key factor to balance printing resolution and stem cell integrity, Adv Healthc Mater 5 (2016) 326–333.
[57] P.L. Blackshear, F.D. Dorman, J.H. Steinbach, Some mechanical effects that influence haemolysis, Trans Am Soc Artif Intern Organs 11 (1965) 112.
[58] M.G. Li, X.Y. Tian, N. Zhu, D.J. Schreyer, X.B. Chen, Modelling process-induced cell damage in the bio-dispensing process, Tissue Eng C Methods 16 (2010) 533–542.
[59] I.T. Ozbolat, Y. Yu, Bioprinting toward organ fabrication: challenges and future trends, IEEE Trans Biomed Eng 60 (3) (2013) 691–699.
[60] M. McCune, A. Shafiee, G. Forgacs, I. Kosztin, Predictive modelling of post bioprinting structure formation, Soft Matter 10 (11) (March 21, 2014) 1790–1800.
[61] A. Shafiee, M. McCune, G. Forgacs, I. Kosztin, Post-deposition bioink self-assembly: a quantitative study, Biofabrication 7 (4) (November 5, 2015) 045005, https://doi.org/10.1088/1758-5090/7/4/045005.
[62] E. Flenner, L. Janosi, B. Barz, A. Neagu, G. Forgacs, I. Kosztin, Phys Rev E Stat Nonlinear Soft Matter Phys 85 (2012) 031907.
[63] K. Jakab, A. Neagu, V. Mironov, R.P. Markwald, G. Forgacs, Engineering biological structures of prescribed shape using selfassembling multicellular systems, Proc Natl Acad Sci USA 101 (2004) 2864–2869.
[64] K. Jakab, B. Damon, A. Neagu, A. Kachurin, G. Forgacs, Three-dimensional tissue constructs built by bioprinting, Biorheology 43 (2006) 509–513.
[65] K. Jakab, C. Norotte, B. Damon, F. Marga, A. Neagu, C.L. Besch- Williford, A. Kachurin, K.H. Church, H. Park, V. Mironov, R. Markwald, G. Vunjak-Novakovic, G. Forgacs, Tissue engineering by self-assembly of cells printed into topologically defined structures, Tissue Eng 14 (3) (2008) 413–421.
[66] F. Marga, A. Neagu, I. Kosztin, G. Forgacs, Developmental biology and tissue engineering, Birth Defects Res C 81 (2007) 320–328.
[67] A. Neagu, K. Jakab, R. Jamison, G. Forgacs, Role of physical mechanisms in biological self-organization, Phys Rev Lett 95 (2005) 178104.

[68] A. Neagu, I. Kosztin, K. Jakab, B. Barz, M. Neagu, R. Jamison, G. Forgacs, Computational modelling of tissue self-assembly, Mod Phys Lett B 20 (20) (2006) 1217–1231.
[69] Y. Sun, X. Yang, Q. Wang, In-silico analysis on biofabricating vascular networks using kinetic Monte Carlo simulations, Biofabrication 6 (1) (March 2014) 015008.
[70] X. Yang, V. Mironov, Q. Wang, Modeling fusion of cellular aggregates in biofabrication using phase field theories, J Theor Biol 303 (June 21, 2012) 110–118, https://doi.org/10.1016/j.jtbi.2012.03.003.
[71] A.R. Patrachari, J.T. Podichetty, S.V. Madihally, Application of computational fluid dynamics in tissue engineering, J Biosci Bioeng 114 (2) (2012) 123–132.
[72] M. Cioffi, F. Boschetti, M.T. Raimondi, G. Dubini, Modelling evaluation of the fluid-dynamic microenvironment in tissue-engineered constructs: a micro-CT based model, Biotechnol Bioeng 93 (2006) 500–510.
[73] C. Jungreuthmayer, S.W. Donahue, M.J. Jaasma, A.A. Al-Munajjed, J. Zanghellini, D.J. Kelly, et al., A comparative study of shear stresses in collagen-glycosaminoglycan and calcium phosphate scaffolds in bone tissue-engineering bioreactors, Tissue Eng 15 (2009) 1141–1149.
[74] F. Maes, T. Claessens, M. Moesen, H. Van Oosterwyck, P. Van Ransbeeck, P. Verdonck, Computational models for wall shear stress estimation in scaffolds: a comparative study of two complete geometries, J Biomech 45 (2012) 1586–1592.
[75] M.T. Raimondi, F. Boschetti, L. Falcone, F. Migliavacca, A. Remuzzi, G. Dubini, The effect of media perfusion on three-dimensional cultures of human chondrocytes: integration of experimental and computational approaches, Biorheology 41 (2004) 401–410.
[76] R. Voronov, S. Van Gordon, V.I. Sikavitsas, D.V. Papavassiliou, Computational modelling of flow-induced shear stresses within 3D salt-leached porous scaffolds imaged via micro-CT, J Biomech 43 (2010) 1279–1286.
[77] S. Truscello, G. Kerckhofs, S. Van Bael, G. Pyka, J. Schrooten, et al., Prediction of permeability of regular scaffolds for skeletal tissue engineering: a combined computational and experimental study, Acta Biomater 8 (2012) 1648–1658. 22210520.
[78] R.J. McCoy, F.J. O'Brien, Visualizing feasible operating ranges within tissue engineering systems using a "windows of operation" approach: a perfusion-scaffold bioreactor case study, Biotechnol Bioeng 109 (2012) 3161–3171.
[79] V.I. Sikavitsas, G.N. Bancroft, J.J. Lemoine, M.A.K. Liebschner, M. Dauner, A.G. Mikos, Flow perfusion enhances the calcified matrix deposition of marrow stromal cells in biodegradable nonwoven fiber mesh scaffolds, Ann Biomed Eng 33 (2005) 63–70.
[80] I. Papantoniou, Y.C. Chai, F.P. Luyten, J. Schrooten, Process quality engineering for bioreactor-driven manufacturing of tissue-engineered constructs for bone regeneration, Tissue Eng C Methods 19 (2013) 596–609.
[81] I. Papantoniou, M. Sonnaert, L. Geris, F.P. Luyten, J. Schrooten, G. Kerckhofs, Three-dimensional characterization of tissue-engineered constructs by contrast-enhanced nano-focus computed tomography, Tissue Eng C Methods 20 (2014) 177–187.
[82] A. Lesman, Y. Blinder, S. Levenberg, Modelling of flow-induced shear stress applied on 3D cellular scaffolds: implications for vascular tissue engineering, Biotechnol Bioeng 105 (2010) 645–654.
[83] I. Papantoniou, Y. Guyot, M. Sonnaert, G. Kerckhofs, F.P. Luyten, L. Geris, et al., Spatial optimization in perfusion bioreactors improves bone tissue-engineered construct quality attributes, Biotechnol Bioeng 111 (12) (2014) 2560–2570. https://doi.org/10.1002/bit.25303.
[84] Y. Guyot, F.P. Luyten, J. Schrooten, I. Papantoniou, L. Geris, A three–dimensional computational fluid dynamics model of shear stress distribution during neotissue growth in a perfusion bioreactor, Biotechnol Bioeng 112 (2015) 2591–2600. https://doi.org/10.1002/bit.25672.

[85] Y. Guyot, I. Papantoniou, F.P. Luyten, L. Geris, Coupling curvature-dependent and shear stress-stimulated neotissue growth in dynamic bioreactor cultures: a 3D computational model of a complete scaffold, Biomech Model Mechanobiol 15 (2016) 169. https://doi.org/10.1007/s10237-015-0753-2.
[86] C. Williams, O.E. Kadri, R.S. Voronov, V.I. Sikavitsas, Time-dependent shear stress distributions during extended flow perfusion culture of bone tissue engineered constructs, Fluid 3 (2) (2018) 25, https://doi.org/10.3390/fluids3020025.
[87] K. Wuertz, K. Godburn, J.C. Iatridis, MSC response to pH levels found in degenerating intervertebral discs, Biochem Biophys Res Commun 379 (2009) 824–829.
[88] L.E. Monfoulet, P. Becquart, D. Marchat, K. Vandamme, M. Bourguignon, E. Pacard, et al., The pH in the microenvironment of human mesenchymal stem cells is a critical factor for optimal osteogenesis in tissue-engineered constructs, Tissue Eng 20 (2014) 1827–1840.
[89] M.S. Hossain, D.J. Bergstrom, X.B. Chen, Prediction of cell growth rate over scaffold strands inside a perfusion bioreactor, Biomech Model Mechanobiol 14 (2) (2014) 333–344, https://doi.org/10.1007/s10237-014-0606-4.
[90] M.S. Hossain, D.J. Bergstrom, X.B. Chen, Modelling and simulation of the chondrocyte cell growth, glucose consumption and lactate production within a porous tissue scaffold inside a perfusion bioreacto, Biotechnol Rep 5 (2015) 55–62.
[91] M.M. Nava, M.T. Raimondi, R. Pietrabissa, A multiphysics 3D model of tissue growth under interstitial perfusion in a tissue-engineering bioreactor, Biomech Model Mechanobiol 12 (6) (November 2013) 1169–1179, https://doi.org/10.1007/s10237-013-0473-4.
[92] R.A. Fisher, The arrangement of field experiments, J Ministry Agric Great Britain 33 (1926) 503–513.
[93] K. Desai, C. Sung, DOE optimization and phase morphology of electrospun nanofibers of PANI/PMMA blends, NSTI Nanotechnol 3 (2004) 429–432.
[94] A. Nazir, N. Khenoussi, L. Schacher, T. Hussain, D. Adolphe, A.H. Hekmati, Using the Taguchi method to investigate the effect of different parameters on mean diameter and variation in PA-6 nanofibres produced by needleless electrospinning, RSC Adv 5 (2015) 76892–76897.
[95] F.A.A. Ruiter, C. Alexander, F.R.A.J. Rose, J.I. Segal, A design of experiments approach to identify the influencing parameters that determine poly-D,L-lactic acid (PDLLA) electrospun scaffold morphologies, Biomed Mater 12 (5) (September 25, 2017) 055009, https://doi.org/10.1088/1748-605X/aa7b54.
[96] P. Sheshadri, R.A. Shirwaiker, Characterization of material–process–structure interactions in the 3D bioplotting of polycaprolactone, 3D Print Addit Manuf 2 (1) (2015). https://doi.org/10.1089/3dp.2014.0025.
[97] P. Ravi, P.S. Shiakolas, J.C. Oberg, S. Faizee, A.K. Batra, On the development of a modular 3D bioprinter for research in biomedical device fabrication, in: ASME International Mechanical Engineering Congress and Exposition, vol. 2A, ASME, 2015, https://doi.org/10.1115/IMECE2015-51555. Advanced Manufacturing:V02AT02A059.
[98] H.A. Almeida, P.J. Bártolo, Topological optimisation of scaffolds for tissue engineering, Procedia Eng. 59 (2013) 298–306.
[99] A. Boccaccio, A.E. Uva, M. Fiorentino, L. Lamberti, G. Monno, A mechanobiology-based algorithm to optimize the microstructure geometry of bone tissue scaffolds, Int J Biol Sci 12 (1) (2016). 26722213.
[100] F. Boukouvala, M.G. Ierapetritou, Surrogate-based optimization of expensive flowsheet modelling for continuous pharmaceutical manufacturing, J Pharm Innov 8 (2) (2013) 131–145.

[101] H.M. Chi, H. Moskowitz, O.K. Ersoy, K. Altinkemer, P.F. Gavin, B.E. Huff, B.A. Olsen, Machine learning and genetic algorithms in pharmaceutical development and manufacturing processes, Decis Support Syst 48 (1) (2009) 69–80. ISSN 0167-9236. https://doi.org/10.1016/j.dss.2009.06.010.
[102] H.J. Kushner, A new method of locating the maximum point of an arbitrary multipeak curve in the presence of noise, J Basic Eng 86 (1) (1964) 97–106.
[103] J. Mockus, Bayesian Approach to Global Optimization: Theory and Applications, Kluwer Academic Publishers, 1989.
[104] J. Nogueira, et al., Unscented Bayesian Optimization for Safe Robot Grasping, IROS, 2016.
[105] J.R. Banga, Optimization in computational systems biology, BMC Syst Biol 2 (1) (2008) 47.
[106] F. Boukouvala, et al., Global optimization advances in mixed-integer nonlinear programming, MINLP, and constrained derivative-free optimization, CDFO, Eur J Oper Res 252 (2016) 701–727.
[107] C.-L. Hwang, A.S.M. Masud, Multiple Objective Decision Making – Methods and Applications: A State-of-the-Art Survey, Springer, 1979.
[108] T.M. Morrison, M.L. Dreher, S. Nagaraja, L.M. Angelone, W. Kainz, The role of computational modeling and simulation in the total product life cycle of peripheral vascular devices, J Med Dev Trans ASME 11 (2) (2017) 024503.
[109] T.M. Morrison, P. Pathmanathan, M. Adwan, E. Margerrison, Advancing regulatory science with computational modeling for medical devices at the FDA's office of science and engineering laboratories, Front Med 5 (2018) 241, https://doi.org/10.3389/fmed.2018.00241.
[110] S. Kyle, Z.M. Jessop, S.P. Tarassoli, A. Al-Sabah, I.S. Whitaker, Assessing printability of bioinks. (Chapter 9), in: 3D Bioprinting for Reconstructive Surgery, 2017, pp. 173–189.
[111] H.V. Unadkat, M. Hulsman, K. Cornelissen, B.J. Papenburg, R.K. Truckenmüller, A.E. Carpenter, M. Wessling, G.F. Post, M. Uetz, M.J. Reinders, D. Stamatialis, C.A. van Blitterswijk, J. de Boer, An algorithm-based topographical biomaterials library to instruct cell fate, Proc Natl Acad Sci USA 108 (40) (2017) 16565–16570.
[112] F. Sefat, A. Atala, M. Mozafari, An introduction to tissue engineering scaffold. (Chapter 1), in: F. Sefat, A. Atala, M. Mozafari (Eds.), The Handbook for Tissue Engineering Scaffolds, Elsevier, 2019.
[113] J.P. St-Pierre, Fabrication techniques of tissue engineering scaffolds. (Chapter 6), in: F. Sefat, A. Atala, M. Mozafari (Eds.), The Handbook for Tissue Engineering Scaffolds, Elsevier, 2019.